ISSN 1061-8309, Russian Journal of Nondestructive Testing, 2020, Vol. 56, No. 5, pp. 452–459. © Pleiades Publishing, Ltd., 2020.
Russian Text © The Author(s), 2020, published in Defektoskopiya, 2020, No. 5, pp. 52–59.

OPTICAL METHODS

Fast Nondestructive Technique for Analyzing Deflection of Membranes Located on the Substrate

A. A. Dedkova[a], *, N. A. Dyuzhev[a], E. E. Gusev[a], and M. Yu. Shtern[a]

[a] *National Research University of Electronic Technology (MIET), Zelenograd, Moscow, 124498 Russia*

**e-mail: dedkova@ckp-miet.ru*

Received October 8, 2019; revised February 19, 2020; accepted March 13, 2020

Abstract—We describe a nondestructive technique for automated analysis of deflection of substrate-mounted membrane structures, which are a key element of devices based on microelectromechanical systems (MEMS devices). The technique includes analysis of substrates with an optical profiler operating in a specialized mode and mathematical processing of measurement results. The technique allows determining the magnitude and sign of deflection of membrane structures for each measurement area. The procedure results in grading the value of deflection and detecting the following types of the state of membrane structures, which are important for assessing the yield and reliability of MEMS devices based on these structures: separation or rupture of the structure, its significant deflection, its slight deflection, and lack of a deflection. All results are displayed in map format on the surface of a substrate with membrane structures with the ability to access more detailed data. The developed technique makes it possible to localize regions with a maximum, predetermined, and low yield of suitable crystals of MEMS devices, as well as flawed regions over the entire substrate surface. The use of the technique significantly increases the accuracy and reduces the measurement time for estimating the yield of suitable membrane structures, and also makes it possible to adjust the process route so as to increase the yield of suitable crystals of MEMS devices.

Keywords: nondestructive testing technique, optical profiler, yield of crystals of MEMS devices with membrane structures, interferometry, process route, substrate surface map with various deflection of membrane structures, deformation, relief, mechanical stresses, strength, membrane, deflection

DOI: 10.1134/S1061830920050046

INTRODUCTION

Currently, when manufacturing integrated circuits and MEMS devices, they are striving to optimize as much as possible the measurement process over time and reduce the impact of the human factor on the substrate by automating the process [1]. This can be implemented industrially both by using the capabilities of modern testing equipment and by developing novel automated measuring techniques for traditional monitoring systems. This work is devoted to the implementation of the second approach, namely, to developing an online nondestructive method for monitoring the yield and level of rejection of defective membrane structures of MEMS devices by measuring the deflection of substrate-mounted membranes with an optical profiler operating in a specialized mode, followed by mathematical processing of the measurement results.

The approach described continues the authors' developments in the field of measurement automation, related to the creation and implementation of methods for mapping the surface of substrate and determining local residual mechanical stresses in thin films [2, 3].

The purpose of this work is to develop an fast nondestructive method for monitoring the yield and level of rejection of defective membrane structures of crystals of MEMS devices on the surface of the substrate based on the created hardware-software complex for the fast measurement of membrane deflections.

ANALYSIS OF MEMBRANE STRUCTURES

Crystals with membrane structures are used in many MEMS devices and are produced on silicon wafers using planar technology [4].

For example, in through-target X-ray tubes, the membrane structure is part of the anode assembly [5] and determines the size of the focal spot and the intensity of X-ray radiation. In this case, the membrane

must be strong enough, since the pressure inside the tube is lowered to reduce electron losses; this leads to a pressure drop affecting the membrane anode assembly with possible critical deformation or destruction of the membrane putting the device out of order.

The strength characteristics of membranes are determined using methods based on the analysis of the magnitude of membrane deflection versus the value of overpressure [6–9]. The membrane deflection is the height difference between the maximum-magnitude coordinate point of the membrane relief and the plane of the substrate surface corresponding to the membrane base. To more accurately determine the magnitude of the deflection caused by the pressure applied, it is necessary to pre-measure the initial deflection (caused by residual stresses due to technological processes involved in membrane manufacture). It is important to note that when analyzing the change in the deflection due to the applied pressure, the researchers often neglect the presence of the initial deflection, and, in the vast majority of cases, they do not take into account the features of the initial membrane shape, as should be done for accurate calculation.

Another example is thermal sensors for measuring the flow rate of a gas or air medium based on the effect of temperature-induced changes in the electrical resistance of the heating and measuring resistors mounted on membranes [10]. At the same time, to increase the sensitivity of thermal sensors, the membrane surface should be fairly even (have small deflection).

Thus, in the process of testing the technology of manufacturing MEMS devices with membrane elements [11], the main attention is paid to testing the manufacturing of membrane structures, since their parameters determine the characteristics of the fabricated device.

One of the key operations in creating membrane structures is through etching of silicon wafers from the back through a mask to the dielectric layers formed on the front side of the wafers. In the process of such a deep etching, one often observes insufficient selectivity of the photoresist or aluminum mask to monocrystalline silicon. Also, it is impossible not to note the difficulty of controlling the moment of completion of the etching process of thick (hundreds of micrometers) silicon while maintaining thin (hundreds of nanometers) membrane material.

In this regard, the developers of MEMS devices based on membrane structures are faced with the task of choosing the optimum parameters of technological processes based on testing the characteristics of membrane structures. Currently, similar techniques are being actively developed [12–23].

The use of noncontact methods for monitoring membrane structures on the surface of silicon wafers leads to the optimization of the process route and increases the yield of suitable products [2]. The standard nondestructive method for analyzing membrane structures on a substrate is the analysis of the surface relief of the substrate in the areas where these structures are located, as determined by an optical profiler in the mode of vertical scanning interferometry mode [24, 25]. At the same time, the map of the surface relief is constructed and the deflection of the membrane is determined. This initial deflection is associated with the presence of residual stresses resulting from the technological operations of manufacturing the membrane and affects the operational characteristics of final products.

A sample of several crystals is usually made when evaluating the results of technological operations. Crystals for measurements can be selected both after the operation of dividing the substrate into crystals by the leading batch technologist and on the whole substrate by the operator of the measuring unit. However, all membrane structures on the substrate need to be checked for comprehensive analysis. This will make it possible to construct a substrate map and evaluate the distribution of suitable crystals. Having located regions with satisfactory and unsatisfactory membrane characteristics will allow establishing a correspondence between the features of the process route (unevenness of the processes of formation and etching of films over the substrate area) and the output distribution of the parameters of the structures over the substrate. Also, in the case of a large percentage of defects, an additional layer with tensile or compressive stresses can be introduced into the membranes.

The use of the standard item-by-item technique for analyzing crystals with membrane structures significantly increases the measurement time. It is worth noting that, given the tendency to increase the number of crystals on the wafer (due to a decrease in the size of the elements simultaneously with an increase in the diameter of the wafers [26–35]), this will require significant time expenses of the operator.

It should be noted separately that when using the standard method for determining membrane deflection, the analysis result will differ depending on the choice of the profile line and the cursor position, which are determined manually by the operator. This leads to a decrease in the accuracy and comparability of measurement results in the analysis of the entire substrate.

Thus, the urgent task is to develop and test a procedure for the analysis of membrane structures integrally on all crystals of MEMS devices formed on the substrate. This approach allows one to localize regions with

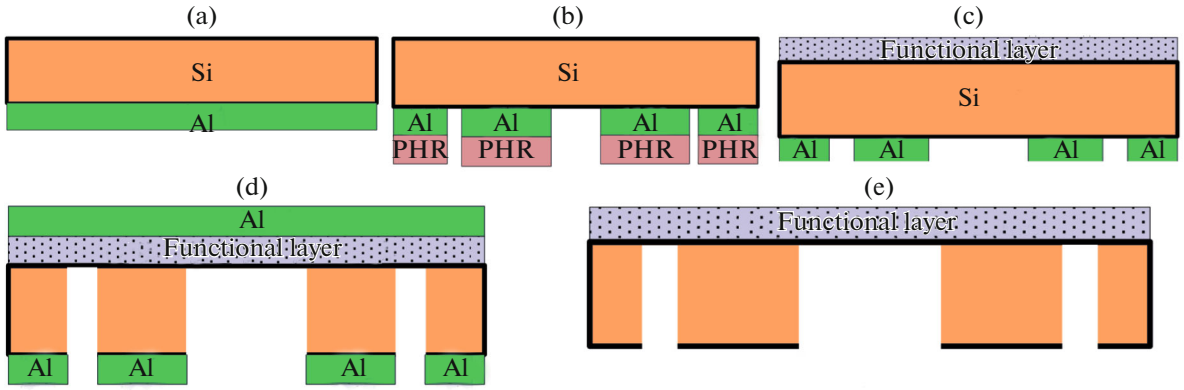

Fig. 1. Process route of manufacturing membrane structures on silicon wafers: (a) after deposition of aluminum layer on the back of wafer; (b) after formation of photoresist mask and etching aluminum layer through this mask; (c) after removal of photoresist mask and deposition of functional layer forming a membrane on the front side of substrate; (d) after through etching of silicon substrate through aluminum mask; (e) final membrane structure after removal of aluminum mask.

maximum yield of suitable crystals and defective areas over the entire substrate surface, significantly reduce the time for the measurement of all crystals, and reduce the influence of the human factor.

The procedure developed by the present authors was tested on a substrate 150 mm in diameter hosting 288 square crystals 6 mm on a side with membrane structures of various diameters. These structures were made according to the process route shown in Fig. 1.

DESCRIPTION OF PROCEDURE

To achieve the goal set, a technique was developed that involves the use of a Veeco Wyko NT 9300 optical profiler. This equipment allows constructing and analyzing a three-dimensional map of the substrate surface in the regions where membrane structures are located (Fig. 2), as well as determining the magnitude of their deflection (Fig. 3). The technique includes recording surface profile in a specialized mode and analyzing membrane deflection using the dedicated software [36].

An algorithm for analyzing a single membrane was developed and was included as a component in the algorithm for analyzing membranes over the entire substrate area. To automate the measurement process, a special grid was constructed on the basis of the Veeco Wyko NT 9300 software, in which the cell sizes correspond to membrane location areas while the full grid dimensions, to the analyzed working area of the substrate. Measurement modes are set in the same way as in the standard case. After starting the measurement process, experimental data are determined that correspond to the coordinates of points on the surface of the analyzed region. The indicated data are saved as separate files for further processing. The number of individual files corresponds to the number of crystals. These files are subsequently used to calculate the magnitude and sign of deflection of membranes using the dedicated software.

For each of the analyzed areas on the surface of the substrate with membranes, it is first necessary to determine the type of the state of membranes. Four membrane-state types were identified in the technique developed. The first type of state is when there are no signs of the relief corresponding to the presence of a membrane with a deflection in the analyzed region, i.e., the region being analyzed is represented by a smooth surface (deflection is less than 1 micron). The second type of state is when the analyzed area is characterized by the presence of a hole, that is, the membrane is destroyed (to be rejected). A membrane with a deflection of 1 to 10 μm corresponds to the third type of state; a membrane with a deflection of more than 10 μm corresponds to the fourth type of state.

The key operations of the membrane analysis algorithm are described below.

First, the leveling operation is performed, which consists in removing the surface slope (Figs. 4a, 4b).

Since experimental data may contain point defects or contaminants, an algorithm is provided to remove such peak surges.

To determine the parameters of membrane structures, it is necessary to initially determine the zone in which the membrane is located. Since the sample cannot be positioned perfectly evenly for measurements, the membrane is displaced relative to the center of the field of view (see Fig. 2). In studies, membranes of various diameters may be present (see Fig. 2), depending on the lithographic pattern used.

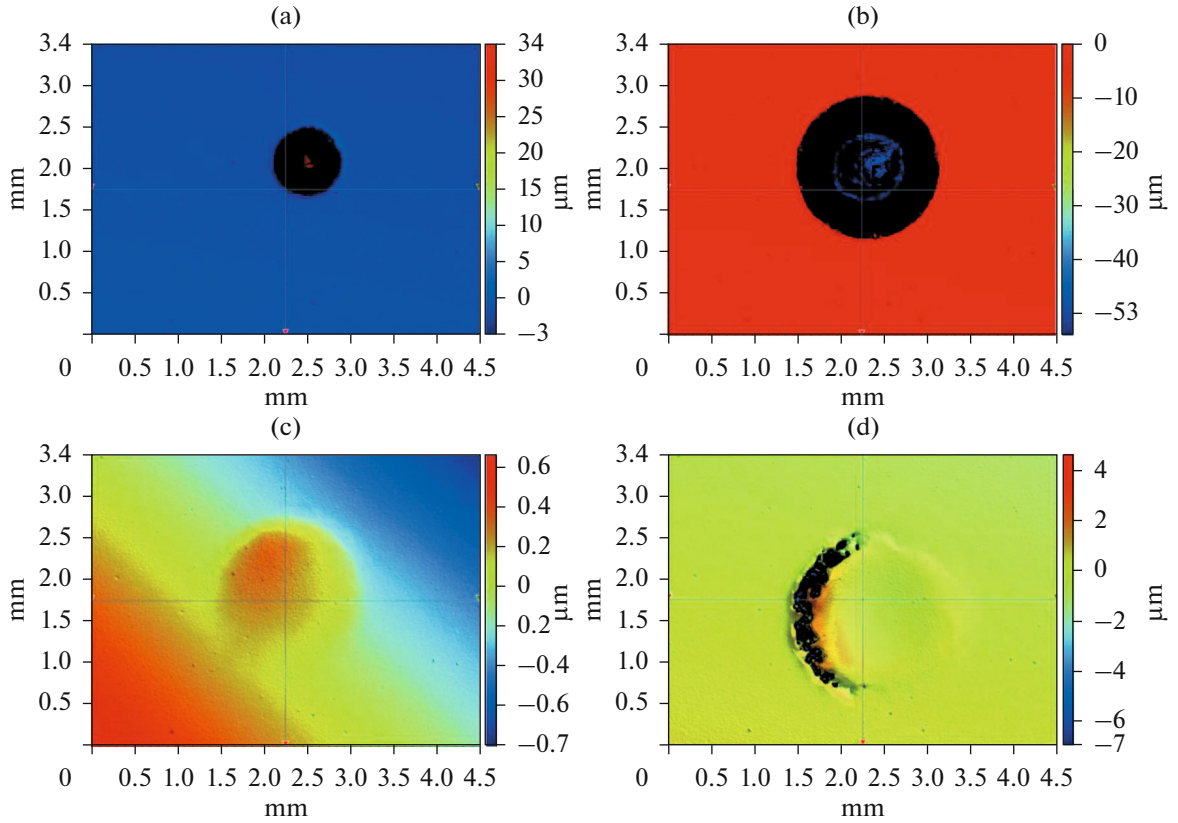

Fig. 2. Images of various membranes obtained using Veeco Wyko NT 9300 optical profiler (membrane-containing surface areas with size on the order of 3.4 × 4.5 mm^2 are shown; color scale corresponds to surface level in microns).

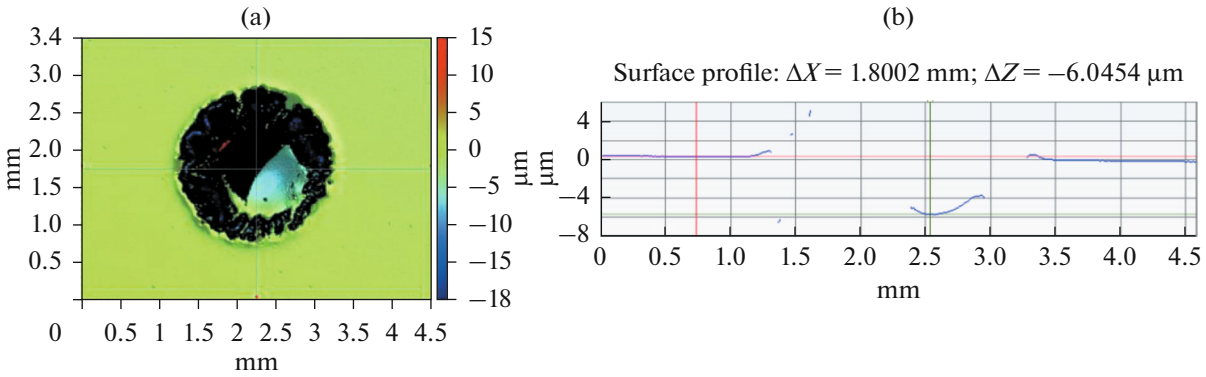

Fig. 3. Image of membrane (a) and surface profile (b) obtained using Veeco Wyko NT 9300 optical profiler.

A membrane with varying type of state is located by comparing the data with the average surface level obtained at the previous step, when leveling the surface; this allows one to determine the boundary areas of membrane structure location.

In the absence of significant data that differ from the average surface level, it is concluded that the analysis area is represented by a smooth surface, that is, membrane state type "1" is detected. Membrane state type "2" is distinguished by the lack of informative data in the assumed region of membrane presence, i.e., uncertain values (Not a Number - NaN) prevail. If state types "1" and "2" have not been detected, then it is concluded that this region contains a membrane structure with nonzero deflection, i.e, membrane state types "3" and "4" are possible.

An important feature of operating the experimental data is partial lack of measurement results (black areas in Figs. 2 and 3a and blank areas in Fig. 3b, corresponding to NaN); this was taken into account

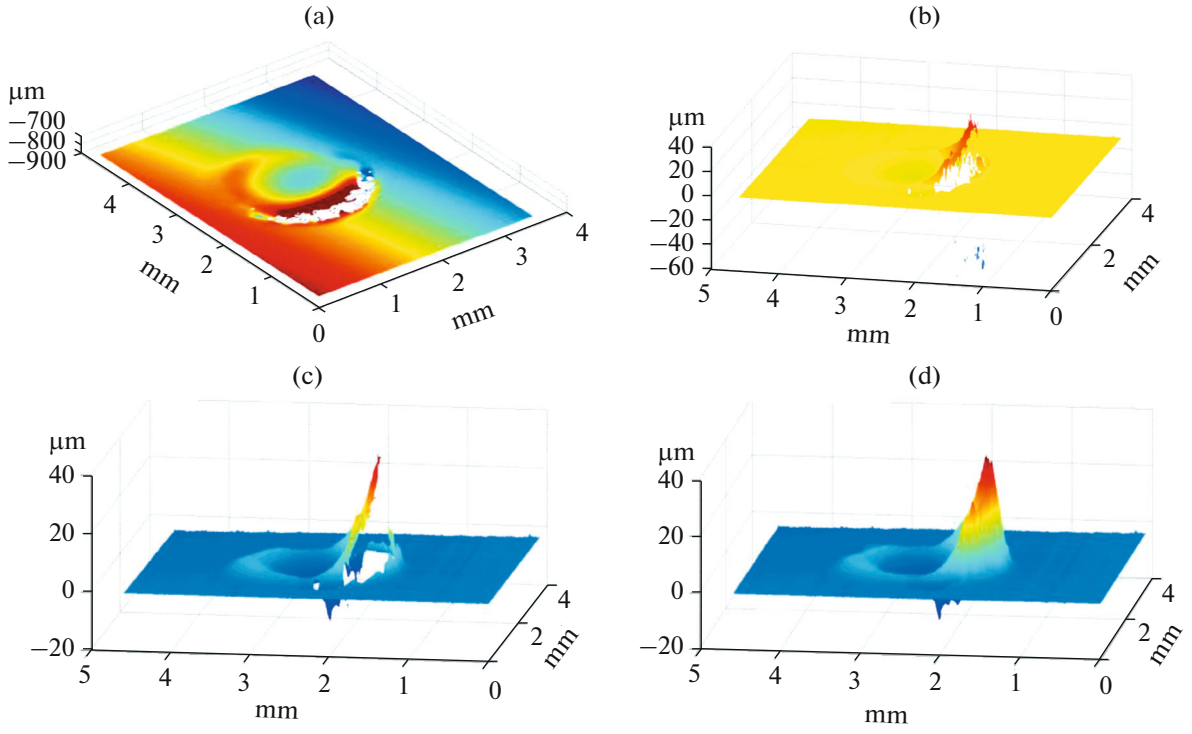

Fig. 4. View of region with membrane: (a) original experimental data, (b) after removal of linear slope, (c) after averaging, (d) after reconstruction of intermediate data.

when analyzing the results. This necessitates not only data averaging and smoothing procedures (Fig. 4c) but also data reconstruction procedures (Fig. 4d).

Then, the deflection is calculated in the assumed zone of the presence of a membrane. The numerical value of deflection is calculated based on the maximum difference, along the vertical axis, between the measured data and the average surface level. In this case, it is taken into account that the maximum deflection should be observed closer to the membrane center. To this end, regions closer to the edge of the membrane are dropped from the analysis so as to cut off a number of uninformative features of the experimental data. The prevailing trend of the convexity or concavity of the membrane structure relief is also determined (see Fig. 3).

When developing the software for analyzing the deflection of membranes on a substrate, it was taken into account that it is important for the operator to be able to obtain a brief summary of all membrane structures on the substrate: the type of state of the membrane (one of the four types of state), as well as the magnitude of deflection and its sign (convexity or concavity). The above information is displayed on screen for all membranes contained on the substrate in a concise and easy-to-read form. An example of the result of calculating the amount of deflection based on the map of the surface of a substrate with membrane structures is shown in Fig. 5.

A visual programming environment was used to accomplish the above task and compile a user-friendly interface. The arrangement of crystals with membranes on the substrate is displayed using a grid. Different colors of grid cells and text allow the operator to quickly assess membrane characteristics. The way the data are presented clearly indicates the location of areas where the membrane is critically deformed.

After analyzing the surface map as a whole, the operator can access more detailed information by clicking on the corresponding grid cell. In this case, the operator gets access to information about the complex shape of the membrane surface, which should later be used for analysis when calculating the membrane strength characteristics.

We analyzed the time required to carry out studies using the standard procedure and the above technique. The process of selecting the measurement region takes $10N$ s for the standard procedure and 10 s for the developed technique (selection of the first measurement region), where N is the number of crystals on the substrate. Moreover, the duration of the process of measurement per se depends on the magnitude of height difference and, on the average, takes approximately $20N$ s in both cases. Initial data analysis takes

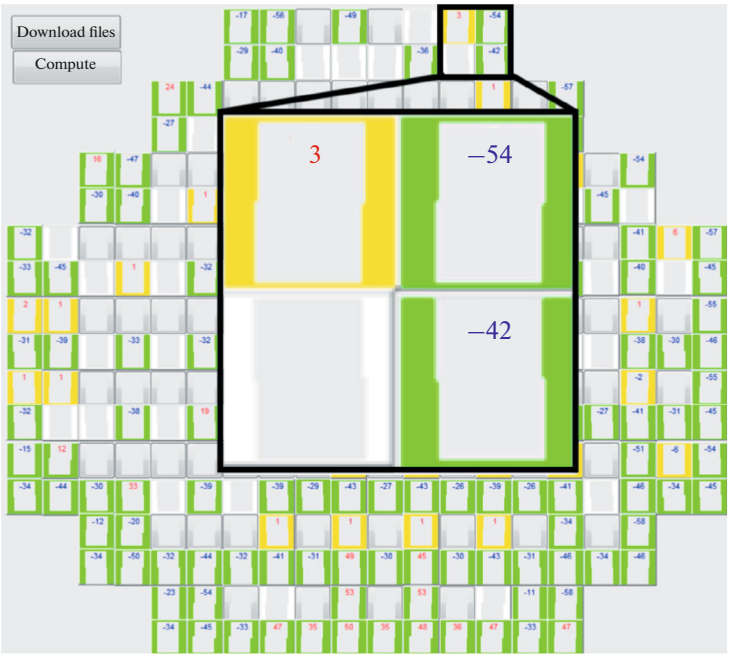

Fig. 5. View of program window with calculated deflection values in microns for all membranes located in grid cells: gray cell is a membrane with no deflection (state type "1"); white cell is a critically deformed membrane (state type "2"); yellow cell is a membrane with a small deflection (state type "3"); green cell is a considerably deflected membrane (state type "4").

approximately $20N$ s for the standard procedure and less than 1 s for the developed technique. Saving data takes approximately $10N$ s for the standard measurement and less than 1 s for the developed technique. In total, it is $(10 + 20 + 20 + 10)\,N$ s, i.e., $60N$ s is the time spent on the measurement of N membrane structures using the standard procedure; $(10 + 20N + 1 + 1)$ s is the time for measuring N membrane structures according to the developed technique. This implies that the measurement time shortens 2–3 times. In this case, the time during which the operator is directly involved in the measurement process with the optical profiler is reduced from the duration of the entire measurement process $60N$ to the duration of the operation of selecting the measurement area of 10 s. The time required to start up the equipment and place the sample is the same in both cases and was not taken into account in the analysis.

CONCLUSIONS

A nondestructive technique has been developed for automated analysis of the deflection of membranes located on a substrate. The technique includes the measurement of membrane structures over the entire substrate area and the automatic determination of deflection across all membranes on the substrate, thus optimizing the subsequent analysis. The use of such techniques becomes an optimum solution when it is necessary to analyze membrane structures over the entire area of the substrate. This approach allows one to localize regions with the maximum yield of the required crystals of MEMS devices and the defective areas over the entire surface of the substrate, while significantly reducing the time it takes to measure all crystals on the substrate. Using this technique allows increasing the accuracy of estimating the yield of suitable membrane structures, as well as adjust process routes of their production so as to increase the yield of suitable crystals.

ACKNOWLEDGMENTS

The authors are grateful to the leading engineer of the Shared Use Center for Microsystems and Electronic Component Base of MIET V.Yu. Kireev for discussing the materials presented in this article and useful comments made.

FUNDING

This work was performed using the equipment of MIET's SUC "Microsystems and Electronic Component Base" with the support of the Ministry of Science and Higher Education of the Russian Federation, agreement 075-15-2019-1650, unique project no. RFMEFI59419X0018.

REFERENCES

1. Bannikov, E.V., The use of PSP in industry, in *International Scientific Review of the Problems and Prospects of Modern Science and Education,* 2019, pp. 25–28.
2. Djuzhev, N.A., Gusev, E.E., Dedkova, A.A., and Makhiboroda, M.A., Non-destructive method of surface mapping to improve accuracy of mechanical stresses measurements, *IOP Conf. Ser.: Mater. Sci. Eng.,* 2018, vol. 289(1), p. 012007. https://doi.org/10.1088/1757-899X/289/1/012007
3. Djuzhev, N.A., Dedkova, A.A., Gusev, E.E., Makhiboroda, M.A., and Glagolev, P.Y., Non-contact technique for determining the mechanical stress in thin films on wafers by profiler, *IOP Conf. Ser.: Mater. Sci. Eng.,* 2016, vol. 189(1), p. 012019. https://doi.org/10.1088/1757-899X/189/1/012019
4. Kireev, V.Yu., *Vvedenie v teoriyu mikroelektroniki i nanotekhnologii* (Introduction to Microelectronics and Nanotechnology), Moscow: FSUE TsNI-IKhM, 2008.
5. Djuzhev, N.A., Makhiboroda, M.A., Preobrazhensky, R.Y., Demin, G.D., Gusev, E.E., and Dedkova, A.A., Development and study of a conceptual model of an X-ray source with a field emission cathode, *J. Surf. Invest.,* 2017, vol. 11(2), pp. 443–448. https://doi.org/10.1134/S1027451017020239
6. Gusev, E.E., Borisova, A.V., Dedkova, A.A., Salnikov, A.A., and Kireev, V.Yu., The effect of ion beam etching on mechanical strength multilayer aluminum membranes, in *Proc. 2019 IEEE Conf. Russ. Young Res. Electr. Electron. Eng., ElConRus,* 2019, vol. 8657243, pp. 1990–1994. https://doi.org/10.1109/EIConRus.2019.8657243
7. Zhao, F., Nonlinear solutions for circular membranes and thin plates, in *Proc. Model. Signal Process. Control Smart Struct.,* 2008, vol. 6926, p. 69260W. https://doi.org/10.1117/12.775511
8. Plaut, R.H., Linearly elastic annular and circular membranes under radial, transverse, and torsional loading. Part I: large unwrinkled axisymmetric deformations, *Acta Mech.,* 2009, vol. 202, pp. 79–99. https://doi.org/10.1007/s00707-008-0037-3
9. Neggers, J., Hoenagels, J.P.M., Hild, F., Roux, S., and Geers, M.G.D., Direct stress-strain measurements from bulged membranes using topography image correlation, *Exp. Mech.,* 2014, vol. 54, no. 5, pp. 717–727. https://doi.org/10.1007/s11340-013-9832-4
10. Bespalov, V.A., Vasil'ev, I.A., Djuzhev, N.A., Mazurkin, N.S., Novikov, D.V., and Popkov, A.F., Modeling primary membrane-type gas-flow-rate transducer, *Izv. Vyssh. Uchebn. Zaved. Elektron.,* 2014, no. 3 (107), pp. 50–56.
11. Dyuzhev, N.A., Gusev, E.E., Gryazneva, T.A., Dedkova, A.A., Dronova, D.A., Kireev, V.Y., Kirilenko, E.P., Migunov, D.M., Novikov, D.V., Patyukov, N.N., Presnukhina, A.A., Bakun, A.D., and Ermakov, D.S., Fabrication and study of parameters and properties of nanostructured membranes for MEMS devices, *Nanotechnol. Russ.,* 2017, vol. 12, nos. 7–8, pp. 426–437. https://doi.org/10.1134/S1995078017040073
12. Djuzhev, N.A., Gusev, E.E., Dedkova, A.A., and Patiukov, N.N., Determination of mechanical stress in the silicon nitride films with a scanning electron microscope, in *Proc. SPIE Int. Soc. Opt. Eng.,* 2016, p. 1022428. https://doi.org/10.1117/12.2250118
13. Muruganandam, D., Influence of post weld heat treatment in friction stir welding of AA6061 and AZ61 alloy, *Russ. J. Nondestr. Test.,* 2018, vol. 54, no. 4, pp. 294–301. https://doi.org/10.1134/s1061830918040095
14. Volchkov, S.O., Dukhan, A.E., Dukhan, E.I., and Kurlyandskaya, G.V., Computer-aided inspection center for magnetoimpedance spectroscopy, *Russ. J. Nondestr. Test.,* 2016, vol. 52, no. 11, pp. 647–652. https://doi.org/10.1134/s1061830916110097
15. Rudnitsky, V.A., Kren, A.P., and Lantsman, G.A., Determining yield strength of metals by microindentation with a spherical tip, *Russ. J. Nondestr. Test.,* 2019, vol. 55, no. 2, pp. 162–168. https://doi.org/10.1134/S1061830919020098
16. Donati, S. and Martini, G., 3D profilometry with a self-mixing interferometer: analysis of the speckle error, *IEEE Photonics Technol. Lett.,* 2019, vol. 31, no. 7, pp. 545–548. https://doi.org/10.1109/LPT.2019.2901274
17. Vairavan, R., Ong, N.R., Sauli, Z., Kirtsaeng, S., Sakuntasathien, S., Shahimin, M.M., Alcain, J.B., Lai, S.L., Paitong, P., and Retnasamy, V., 3D silicon breast surface mapping via structured light profilometry, *AIP Conf. Proc.,* 2017, vol. 1885, no. 1, p. 020252. https://doi.org/10.1063/1.5002446
18. Bazulin, A.E. and Bazulin, E.G., Application of antenna arrays and organosilicon polymers as an immersion medium for ultrasonic testing of objects with rough surfaces, *Russ. J. Nondestr. Test.,* 2014, vol. 50, no. 7, pp. 377–384. https://doi.org/10.1134/s106183091407002x

19. Panjan, P., Cekada, M., Panjan, M., Curkovic, L., and Paskvale, S., Surface density of growth defects in different PVD hard coatings prepared by sputtering, *Vacuum,* 2012, vol. 86, no. 6, pp. 794–798. https://doi.org/10.1016/j.vacuum.2011.07.013
20. Kovalevskaya, Z.G., Uvarkin, P.V., and Tolmachev, A.I., Some features of the formation of the surface microrelief of steel under ultrasonic finishing treatment, *Russ. J. Nondestr. Test.,* 2012, vol. 48, no. 3, pp. 153–158. https://doi.org/10.1134/s1061830912030047
21. Osipov, S.P., Usachev, E.Y., Chakhlov, S.V., Shchetinkin, S.A., and Osipov, O.S., Specific features of material recognition by the multi-energy X-Ray method, *Russ. J. Nondestr. Test.,* 2019, vol. 55, no. 4, pp. 308–321. https://doi.org/10.1134/s1061830919040119
22. Ivina, N.F., Balabaev, S.M., and Tagil'tsev, A.A., Analysis of natural vibrations of round flexing membrane-type piezoelectric transducers with an arbitrary dimension ratio, *Russ. J. Nondestr. Test.,* 2003, vol. 39, no. 8, pp. 589–595.
23. Vladimirov, A.P. and Kapustin, D.S., Comparative Analysis of Dynamic and Holographic Interferometry Methods with Reference to Deformations of a Membrane, *Russ. J. Nondestr. Test.,* 2004, vol. 40, no. 1, pp. 61–65.
24. Jiang, C., Kilcullen, P., Liu, X., Ozaki, T., and Liang, J., Three-dimensional structured light profilometry using a bandwidth-limited projector, *Proc. SPIE Int. Soc. Opt. Eng.,* 2019, vol. 109320, p. 109320K. https://doi.org/10.1117/12.2510145
25. Mao, C-L., Lu, R-S., Dong, J-T., and Zhang, Y-Z., Overview of the 3D profilometry of phase shifting fringe projection, *Jiliang Xuebao/Acta Metrol. Sinica,* 2018, vol. 39, no. 5, pp. 628–640. https://doi.org/10.3969/j.issn.1000-1158.2018.05.07
26. Rhee, H.S., Kim, I.R., Jeong, J.H., Son, N.K., Hong, H.B., Cho, S.I., Park, Y.M., Kim, D.W., Choi, Y.K., Ahn, J.H., Kang, S.G., Yeo, K.H., Kim, J.T., Lee, E.C., Youn, J.M., and Yoon, J.S., 8LPP logic platform technology for cost-effective high volume manufacturing, in *Symp. VLSI Technol.,* 2018, pp. 217–218. https://doi.org/10.1109/VLSIT.2018.8510673
27. Lanzillo, N.A., Motoyama, K., Hook, T., and Clevenger, L., Impact of line and via resistance on device performance at the 5nm gate all around node and beyond, in *IEEE Int. Interconnect Technol. Conf.,* 2018, vol. 8430294, pp. 70–72. https://doi.org/10.1109/IITC.2018.8430294
28. Bae, G., Bhuwalka, K.K., Lee, S-H., Song, M.-G., Jeon, T-S., Kim, C., Kim, W., Park, J., Kim, S., Kwon, U., Jeon, J., Nam, K-J., Lee, S., Lian, S., Seo, K-I., Lee, S-G., Park, J.H., Heo, Y-C., Rodder, M.S., Kittl, J.A., Kim, Y., Hwang, K., Kim, D-W., Liang, M-S., and Jung, E.S., A novel tensile Si (n) and compressive SiGe (p) dual-channel CMOS FinFET co-integration scheme for 5nm logic applications and beyond, *Tech. Dig.—Int. Electron Devices Meet.,* 2017, vol. 7838496, pp. 28.1.1–28.1.4. https://doi.org/10.1109/IEDM.2016.7838496
29. Ming, L., Kyoung, H.Y., Sung, D.S., Yun, Y.Y., Kim, D-W., Tae, Y.C., Kyung, S.O., and Lee,W-S., Sub-10 nm gate all-around CMOS nanowire transistors on bulk Si substrate, *Dig. Tech. Pap.—Symp. VLSI Technol.,* 2009, vol. 5200646, pp. 94–95.
30. Braun, T., Becker, K.-F., Voges, S., Bauer, J., Kahle, R., Bader, V., Thomas, T., Aschenbrenner, R., and Lang, K.-D., 2418 Fan-out panel level packing, in *Proc. Electron. Compon. Technol. Conf.,* 2014, vol. 6897401, pp. 940–946. https://doi.org/10.1109/ECTC.2014.6897401
31. Koitzsch, M., Lewke, D., Schellenberger, M., Pfitzner, L., Ryssel, H., and Zühlke, H-U., Enhancements in resizing single crystalline silicon wafers up to 450 mm by using thermal laser separation, in *ASMC (Adv. Semicond. Manuf. Conf.) Proc.,* 2012., vol. 6212923, pp. 336–341. https://doi.org/10.1109/ASMC.2012.6212923
32. Yang, Y. and Kushner, M.J., 450 mm dual frequency capacitively coupled plasma sources: Conventional, graded, and segmented electrodes, *J. Appl. Phys.,* 2010, vol. 108, no. 11, pp. 113306. https://doi.org/10.1063/1.3517104
33. Fischer, A., Kissinger, G., Load induced stresses and plastic deformation in 450 mm silicon wafers, *Appl. Phys. Lett.,* 2007, vol. 91, no. 11, p. 111911. https://doi.org/10.1063/1.2784964
34. Pettinato, J.S. and Pillai, D., Technology decisions to minimize 450-mm wafer size transition risk, *IEEE Trans. Semicond. Manuf.,* 2005, vol. 18, no. 4, pp. 501–509. https://doi.org/10.1109/TSM.2005.858471
35. Ge, M., Zhu, H., Huang, C., Liu, A., and Bi, W., Investigation on critical crack-free cutting depth for single crystal silicon slicing with fixed abrasive wire saw based on the scratching machining experiments, *Mater. Sci. Semicond. Process.,* 2018, vol. 74, pp. 261–266. https://doi.org/10.1016/j.mssp.2017.10.027
36. Dedkova, A.A. and Dyuzhev, N.A., Data processing program for a series of measurements of membrane structures to determine their deflection and qualitative features. Computer program certificate no. 2019663188.

Translated by V. Potapchouck